

Probing interface magnetism in the FeMn/NiFe exchange bias system using magnetic second harmonic generation

Luiz C. Sampaio, Alexandra Mougin,^y and Jacques Ferre
 Laboratoire de Physique des Solides, UMR CNRS 8502,
 Bât. 510, Université Paris Sud, 91405 Orsay, France

Patrick Georges and Alain Brun
 Laboratoire Charles Fabry de l'Institut d'Optique Théorique et Appliquée (IO TA),
 Bât. 503, UMR CNRS 8501, Université Paris Sud, 91405 Orsay, France

Harry Bemas
 Centre de Spectrométrie Nucléaire et de Spectrométrie de Masse,
 UMR CNRS 8609, Bât. 108, Université Paris Sud, 91405 Orsay, France

Stefan Poppe, Tim Mewes, Jürgen Fassbender, and Burkard Hillebrands
 Fachbereich Physik and Forschungs- und Entwicklungsschwerpunkt Materialwissenschaften,
 Erwin-Schrodinger-Strasse 56, 67663 Kaiserslautern, Germany
 (Dated: March 22, 2024)

Second harmonic generation magneto-optic Kerr effect (SHMOKE) experiments, sensitive to buried interfaces, were performed on a polycrystalline NiFe/FeMn bilayer in which areas with different exchange bias fields were prepared using 5 KeV He ion irradiation. Both reversible and irreversible uncompensated spins are found in the antiferromagnetic layer close to the interface with the ferromagnetic layer. The SHMOKE hysteresis loop shows the same exchange bias field as obtained from standard magnetometry. We demonstrate that the exchange bias effect is controlled by pinned uncompensated spins in the antiferromagnetic layer.

PACS numbers: 33.55.Fi, 75.70.-i, 42.65.-k, 75.30.Gw

The magnetic exchange interaction between an antiferromagnetic (AF) and an adjacent ferromagnetic (F) layer may lead to the exchange bias effect discovered in 1956 [1, 2]. Among other various intriguing features, this effect leads to a shift of the F hysteresis loop along the field axis by the so-called exchange bias field H_{eb} . For recent reviews see Refs. [3, 4, 5]. Proposed models to account for the exchange bias involve (i) domain walls or partial domain walls in the AF layer which are either parallel [5, 6] or perpendicular [7] to the interface, and/or (ii) uncompensated AF layer magnetic moments at the interface [7, 8, 9] and/or in the bulk [9, 10]. In most exchange bias models, the interfacial uncompensated spins are linked to roughness, structural defects, or disoriented grains. Although uncompensated spins have been already evidenced [11], their behavior during the F layer magnetic reversal has not been reported so far and, experimentally, the relationship between uncompensated spins and exchange bias is still unclear. In the special case where artificial random defects can be introduced in the AF layer (such as in a diluted antiferromagnet), the so-called "domain state model" [9, 10] showed that the exchange bias effect stems from the volume AF spin arrangement triggered by non-magnetic defects. In this model, AF interfacial reversible and irreversible uncompensated spins (creating $M_{\text{rev}}^{\text{F=AF}}$ and $M_{\text{irr}}^{\text{AF}}$ respectively) are distinguished. Some of the interfacial AF uncompensated spins reverse under the action of an external mag-

netic field and the additional effective interface exchange field originating from the magnetized F layer, whereas the rest of the AF uncompensated spins remain frozen in the same range of applied fields. The reversible uncompensated spins hysteresis loop is found to be shifted along the field axis by H_{eb} and along the magnetization axis by an amount directly proportional to $M_{\text{irr}}^{\text{AF}}$, which scales with H_{eb} [10]. Using superconducting quantum interference device magnetometry, this vertical shift of the hysteresis loop of F/AF bilayers has already been measured and related to the exchange bias field sign [12], although its origin was not determined.

Here we study the second-harmonic magneto-optic Kerr effect (SHMOKE) in an exchange-bias system. A second-harmonic signal in centrosymmetric materials is selectively generated at their interfaces due to symmetry breaking, so that the effect only senses about 2 monolayers in the vicinity of flat surfaces / interfaces [13, 14]. In contrast, the standard linear MOKE signal originates mainly from the bulk of the F layers. Generally, the second harmonic optical polarization $P^{(2)}$, generated at a single interface, consists of both magnetic and non-magnetic contributions due to the magnetic optical susceptibility $\chi_m^{(2)}$ (linear with respect to the magnetization M^z) and the non-magnetic one $\chi_{\text{nm}}^{(2)}$ (independent or even with respect to M^z),

$$P_i(2!) = \sum_{j,k} \chi_{ijk}(2!) E_j(1) E_k(1) \quad (1a)$$

$$\chi(2!; M) = \chi_{nm}(2!; M) + \chi_m(2!; M) \quad (1b)$$

$$\chi(2!; M) = \chi_{nm}(2!; M) + \chi_m(2!; M) \quad (1c)$$

where $E_j(1)$ are the electric field components of the incident light and $\chi_{ijk}(2!)$ the second harmonic susceptibility tensor elements. Each surface or interface contributes to the SHMOKE signal so that the measured intensity from an n multilayer is given by the sum of all interfering signals: $I(2!) / \sum_{(a;b)=(1;::;n)} P_a(2!) P_b(2!)$.

In the present study, polycrystalline bilayers of ferromagnetic $Ni_{81}Fe_{19}$ and antiferromagnetic $Fe_{50}Mn_{50}$ were used in order to tailor the exchange bias field by light ion irradiation [15, 16]. Bilayers of 10 nm FeMn and 5 nm NiFe were evaporated on a 15 nm thick Cu buffer layer deposited on a thermally oxidized Si substrate. A thin Cr cover layer protected the samples from oxidation. In order to initialize the unidirectional anisotropy, the samples were heated and then field cooled. This led to a homogeneous exchange bias field H_{eb} of 200 Oe across the sample, as determined from linear MOKE (see Fig. 1a). After preparation, the exchange bias was modified in different areas of the sample using 5 keV He ion irradiation in a fluence range between 9×10^3 and 2×10^6 ions/cm², leading to H_{eb} values between 100 Oe and 350 Oe (see Fig. 2a, full symbols), consistent with previous work [16]. A discussion of the exchange bias field evolution with ion fluence is given in Ref. [16]. Based upon the latter and ion stopping calculations [17] we note that the interface roughness is not affected when ion fluences are below a few times 10^{16} ions/cm².

SHMOKE experiments were performed with a mode-locked Ti:Sapphire laser operating at a central wavelength of 800 nm, emitting light pulses of width 100 fs at a repetition rate of 86 MHz. All experiments were performed in reflection; the average power at the sample surface was 50 mW within a focus of 30–40 μ m. Using a P-polarized laser beam (P_{in}) at an incident angle of 45° the SH signal can be measured in the transverse configuration (T), and in the longitudinal one (L) when combined with a polarization analysis. The complex effective magnetic and non-magnetic susceptibilities χ_m and χ_{nm} which enter the calculation of the SHMOKE intensity are functions of $\chi_{ijk}(2!)$ tensor elements depending on the measurement geometry, hence they differ in the transverse or longitudinal configurations [13]. In order to extract information on the magnetization at the F/AF interface, the SH contribution of each individual interface and surface (Cu/FeMn, FeMn/NiFe, NiFe/Cr and Cr/air) must be analyzed. Due to the same crystallographic structure and the close chemical nature of the FeMn and NiFe layers, independent of the measurement configuration, χ_{nm}

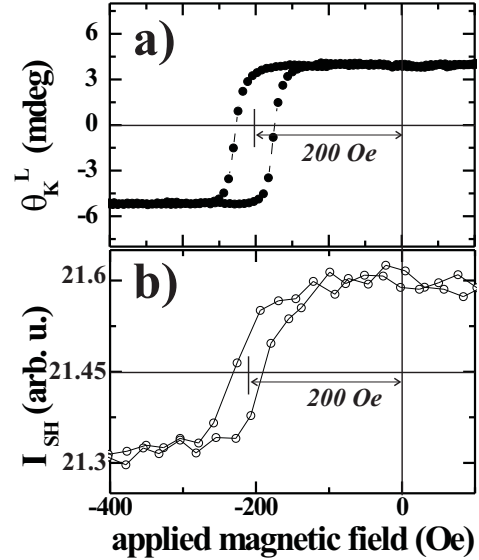


FIG. 1: Bulk and interfacial magnetization reversal loops investigated by linear MOKE (a), and second harmonic MOKE (b), respectively. θ_K^L is the linear Kerr rotation and I_{SH} is the SHMOKE intensity in the transverse configuration.

originating from the FeMn/NiFe interface has a smaller value than those of the upper NiFe/Cr and Cr/air interfaces. Therefore (see definition of $R_L = \frac{j_{nm}^m}{j_{nm}}$ in Eq. (3b)), most of the magnetic SH signal originates from the FeMn/NiFe interface whose R_L is large. No signal is expected from the bulk centrosymmetric F or AF layers [13].

In transverse geometry, with P-polarized incident light, the SH outgoing beam is still P-polarized. Thus, the second harmonic intensity was measured as a function of the applied field, which was oriented perpendicular to the plane of incidence and parallel to the exchange bias direction. The resulting hysteresis loop is shifted along the field axis by the same bias as that of the bulk F layer (Figure 1b). We conclude that SHMOKE selectively probes reversible ($M_{rev}^{F=AF}$) uncompensated spins at the interface, which are coupled to the F layer [9, 10]. Moreover, due to some frustration at the F/AF interface, the SHMOKE hysteresis loop is broader than its bulk F layer counterpart. As shown in Fig. 2a, at all fluences the exchange bias field values measured via SH or linear MOKE agree within the error bars.

Another magnetization term (M_{irr}^{AF}), required to induce any H_{eb} and which remains unaffected by the F layer reversal (between H_c , with $H_c = H_{sat}^F$), has been probed as follows. In order to separate out the magnetic and non-magnetic contributions (see Eq. (1)), the ion fluence dependence of the non-magnetic contribution was first determined. Commonly [18] since the magnetic

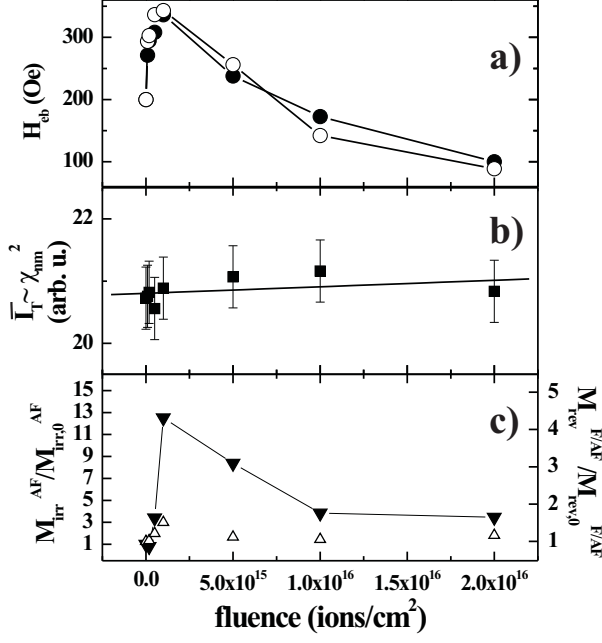


FIG. 2: Ion fluence dependence of: a) exchange bias field (full symbols: M O K E, open symbols: SH M O K E), b) non-magnetic contribution to the SHMOKE signal (I_T), and c) irreversible ($M_{irr}^{AF}/M_{irr,0}^{AF}$, full triangles) and reversible magnetization ($M_{rev}^{F=AF}/M_{rev,0}^{F=AF}$, empty triangles), normalized to their initial value and deduced from asymmetry measurement in the longitudinal configuration. Solid lines are guides to the eye.

term is small as compared to the average part of the SH intensity [19], the non-magnetic contribution scales with the average transverse SHMOKE intensity $\overline{I_T}$ [20]:

$$\overline{I_T} = \frac{I_T(2!; +H) + I_T(2!; H)}{2} \quad (2a)$$

$$/ \left(j_{nm}^2 + j_m^2 \right) \quad (2b)$$

and are the effective Fresnel factors [20]. $\overline{I_T}$ (and thus the effective non-magnetic optical susceptibility j_{nm}^2) is shown in Fig. 2b as a function of ion fluence. Practically no evolution is observed, confirming that no significant interface broadening occurs upon irradiation in this fluence range.

Polarization measurements were performed in the longitudinal configuration, and the magnetic contributions to the SH signal were extracted from the asymmetry $A_L(H; \Psi)$, defined as the normalized intensity difference when the F magnetization is reversed [13]. At the F/AF interface, the structural (n_m) and two distinct magnetic ($j_m(M_{rev}^{F=AF})$ and $j_m(M_{irr}^{AF})$) contributions can give rise to a second harmonic signal. Each magnetic contribution induces a rotation of the polarization of the outgoing beam (from P to S) [13] and is phase shifted relative to

the structural term: δ_{rev} (respectively δ_{irr}) is the phase angle between $j_m(M_{rev}^{F=AF})$ (respectively $j_m(M_{irr}^{AF})$) and n_m . Usually, when the applied field is reversed, all magnetic contributions (linear with M) to the second harmonic polarization change sign. Here, between H , we assume that $M_{rev}^{F=AF}$ reverses i.e. $j_m(M_{rev}^{F=AF})$ changes its sign whereas M_{irr}^{AF} is pinned i.e. $j_m(M_{irr}^{AF})$ does not change. This leads to the following expression of A_L :

$$A_L(H; \Psi) = \frac{I(2!; +H) - I(2!; H)}{I(2!; +H) + I(2!; H)} \quad (3a)$$

$$= \frac{2R_L^{rev} R_L^{irr} \cos(\delta_{rev} - \delta_{irr}) \tan^2 \Psi + 2R_L^{rev} \tan \Psi \cos \delta_{rev}}{1 + (R_L^{rev2} + R_L^{irr2}) \tan^2 \Psi + 2R_L^{irr} \tan \Psi \cos \delta_{irr}} \quad (3b)$$

where Ψ is the analyzer angle and $R_L^{rev} = j_m(M_{rev}^{F=AF})/n_m$ (correspondingly, $R_L^{irr} = j_m(M_{irr}^{AF})/n_m$). Experimentally, for each analyzer angle Ψ , the SH intensity is measured upon reversal of the F layer. This enables us to determine $A_L(\Psi)$. Examples are shown in Fig. 3.

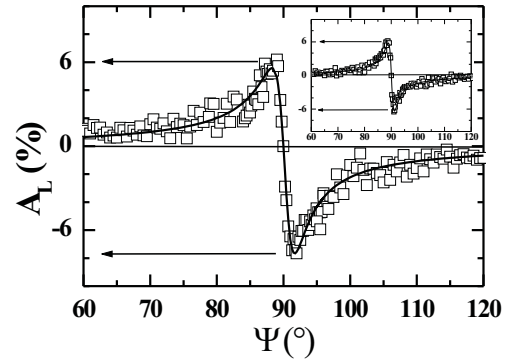


FIG. 3: SHMOKE asymmetry A_L in longitudinal geometry as a function of the analyzer angle Ψ at a fluence of 10^{15} He ions/cm² (10^{16} He ions/cm² in the inset). The solid line is the fit described in the text.

Due to the irreversible term and according to Eq. (3b), two distinct absolute extrema values are evidenced. The difference between them depends on the bias field (it is lower for smaller biases as shown in the inset). By fitting the asymmetry A_L with Eq. (3b), R_L^{rev} and R_L^{irr} are obtained. Since the effective non-magnetic contribution to the second-harmonic generation signal is constant [21], $j_m(M_{irr}^{AF}) = n_m$ (respectively $j_m(M_{rev}^{F=AF}) = n_m$) is directly proportional to M_{irr}^{AF} (respectively $M_{rev}^{F=AF}$) along the magnetic field direction [13].

Our key experimental results (Fig. 2c) are as follows: i) the ion fluence dependence of the irreversible uncompensated spins (full triangles) reproduces that of the exchange bias field (Fig. 2a), ii) a 13-fold increase in the irreversible magnetization and the one order of magnitude smaller interfacial magnetic component enhancement (empty triangles) result in a bias field en-

hancement by a factor of 1.8, iii) the proportion of irreversible (compared to reversible) spins given by the ratio $m(M_{\text{irr}}^{\text{AF}}) = m(M_{\text{rev}}^{\text{F=AF}})$ can reach about 10%. In the same uence regime, the linear Kerr rotation due to the bulk F layer is constant [16]. The uence behavior of $M_{\text{irr}}^{\text{AF}}$ and H_{eb} indicates that pinned uncompensated spins in the AF layer control the bias eld. Moreover, this rigid AF moment is much smaller than the reversible magnetization (maximum ca. 10%). According to the domain state model [9, 10], the exchange bias eld is $H_{\text{eb}} = J_{\text{int}} M_{\text{irr}}^{\text{AF}} = t$, with J_{int} the interface coupling, the magnetic moment per atom and t the F layer thickness. Random exchange defects or antisites are formed in the AF layer via diluting impurities or irradiation. Under the action of the exchange eld originating from the magnetized F layer, the AF domain structure is triggered and the uncompensated spins associated to such defects exhibit an excess magnetization. The latter is presumably reversible in the vicinity of the F layer and pinned if deeper in the AF layer. In the domain state model, both interface coupling and magnetic moment are assumed to be fixed and dilution only drives $M_{\text{irr}}^{\text{AF}}$. In our experimental findings, additional information regarding the interfacial contribution is obtained; changes in local chemical order due to irradiation lead to a slight evolution of the interfacial reversible magnetization. This mixing effect counteracts the increase of $M_{\text{irr}}^{\text{AF}}$ and – for uences larger than those investigated here – reduces the bias as reported in Ref [16].

To obtain insight on the exchange bias mechanism, we have combined ion irradiation-induced tuning of the irreversible magnetization in the AF layer with interface-selective second-harmonic magneto-optic Kerr detection. Our main results do not rely on the technique used to tune the uncompensated spins: whereas in irradiated AF (as in diluted AF), the surplus magnetization is linked to artificially introduced defects, this pinned component may be associated with such natural structural imperfections as grain boundaries in standard F/AF bilayers. Finally, we conclude that the irreversible uncompensated AF spins (wherever they are pinned) drive the exchange bias eld.

The stay of L.C.S. at Orsay was financially supported by CNPq/Brazil. B.H. acknowledges support by CNRS for a sabbatical stay in Orsay. Partial support by the Deutsche Forschungsgemeinschaft is gratefully acknowledged. T.M. acknowledges support by the Studienstiftung des deutschen Volkes.

On leave from Centro Brasileiro de Pesquisas Físicas Rua Dr. Xavier Sigaud, 150 Uca, Rio de Janeiro, RJ 22 290-180

^y Electronic address: mougina@lps.u-psud.fr

- [1] W.H. Meiklejohn and C.P. Bean, Phys. Rev. 102, 1413 (1956).
- [2] W.H. Meiklejohn and C.P. Bean, Phys. Rev. 105, 904 (1957).
- [3] J. Nogues and I.K. Schuller, J. Magn. Mater. 192, 203 (1999).
- [4] A.E. Berkowitz and K. Takano, J. Magn. Mater. 200, 552 (1999).
- [5] R.L. Stamps, J. Phys. D: Appl. Phys. 33, R247 (2000).
- [6] D. Mauri, H.C. Siegmann, P.S. Bagus, and E. Kay, J. Appl. Phys. 62, 3047 (1987).
- [7] A.P. Malozemov, Phys. Rev. B 35, 3679 (1987).
- [8] T.C. Schulthess and W.H. Butler, J. Appl. Phys. 85, 5510 (1999).
- [9] U. Nowak, A. M. Israel, and K.D. Usadel, J. Magn. Mater. 240, 243 (2002).
- [10] U. Nowak, K.D. Usadel, J. Keller, P. Miltenyi, B. Beschoten, and G. Güntherodt, Phys. Rev. B 66, 014430+0014431 (2002).
- [11] W.J. Antel, J.F. Perjeru, and G.R. Harp, Phys. Rev. Lett. 83, 1439 (1999).
- [12] J. Nogues, C. Leighton, and I. Schuller, Phys. Rev. B 61, 1315 (2000).
- [13] K.H. Bennemann, Non linear optics in metals (Clarendon Press Oxford, 1998), chap. 2 and 3.
- [14] H.A. Wierenga, W. de Jong, M.J. Prins, T. Rasing, R. Vollmer, A. Kirilyuk, H. Schwabe, and J. Kirschner, Phys. Rev. Lett. 74, 1462 (1995).
- [15] A. Mougina, T. Mewes, R. Lopusnik, J. Fassbender, B. Hillebrands, M. Jung, D. Engel, A. Ehrenmann, and H. Schmoranzer, IEEE Transactions on Magnetics 36, 2647 (2000).
- [16] A. Mougina, T. Mewes, M. Jung, D. Engel, A. Ehrenmann, H. Schmoranzer, J. Fassbender, and B. Hillebrands, Phys. Rev. B 63, 060409R (2001).
- [17] J.F. Ziegler, J.P. Biersack, and U. Littmark, The Stopping and Range of Ions in Solids (Pergamon, New York, Oxford, <http://www.srim.org/>, 1985).
- [18] J. Hohfeld, E. M. Atthias, R. K. Norren, and K. H. Bennemann, Phys. Rev. Lett. 78, 4861 (1997).
- [19] Experimentally, see Fig. 1b, where the magnetic signal is 1.5% of the average SH signal in transverse.
- [20] J. Gudde, U. Conrad, V. Jahnke, and E. M. Atthias, Phys. Rev. B 59, 6608 (1999).
- [21] The tensor elements entering j_{nm} obtained from Fig. 1b differ from those entering j_{nm} but their dose dependence must be the same.